International Journal of Chronic Obstructive Pulmonary Disease

Dovepress
Taylor & Francis Group

Open Access Full Text Article

ORIGINAL RESEARCH

The Crucial Role of the PPAR Signaling Pathway in the Diagnosis and Treatment of Chronic Obstructive Pulmonary Disease: An Analysis of Gene Expression and Macrophage Polarization

Ling Zhang*, Rong Guo*, Haixia Wu, Abula Abudusalamu, Wei Ding, Dewei Li, Xuemei Wei, Lin Niu

Department of Respiratory and Critical Care Medicine, People's Hospital of Xinjiang Uygur Autonomous Region, Urumqi, 830001, People's Republic of China

*These authors contributed equally to this work

Correspondence: Xuemei Wei; Lin Niu, Department of Respiratory and Critical Care Medicine, People's Hospital of Xinjiang Uygur Autonomous Region, No. 91 Tianchi Road, Tianshan District, Urumqi, 830001, People's Republic of China, Tel +86-13579846469; +86-1319989525, Email wu1208522@163.com; 363141843@qq.com

Purpose: To explore the role of the peroxisome proliferator-activated receptor (PPAR) signaling pathway in chronic obstructive pulmonary disease (COPD) and identify potential biomarkers and therapeutic targets, given that COPD is a major global health burden and the specific molecular mechanisms of the PPAR pathway in COPD are not fully understood.

Patients and Methods: Gene expression data from the GEO database were analyzed to identify key genes and immune cells related to COPD. Peripheral blood samples were collected from COPD patients and healthy controls. Key genes were confirmed by PCR, and immune cells were characterized using flow cytometry.

Results: Eight core genes associated with the PPAR signaling pathway were identified. NCOA1 and PPARGC1A were downregulated in COPD patients, while NCOR1, NRIP1, and SLC27A5 were upregulated. Receiver operating characteristic (ROC) curve analysis showed that NCOA1, NCOR1, and SLC27A5 have potential for COPD diagnosis. There was a significant increase in the proportion of M2 macrophages in COPD patients, indicating a shift in macrophage polarization towards the M2 phenotype. Genes within the PPAR signaling pathway were closely associated with macrophage polarization state.

Conclusion: The research findings provide new biomarkers and potential therapeutic targets for the early diagnosis and personalized treatment of COPD, emphasizing the significant role of the PPAR signaling pathway in the pathogenesis of COPD.

Clinical Trial Registry: The population study involved in this research has been registered under the (chictr.org.cn). Registry identifier: ChiCTR2400086268.

Keywords: COPD, PPAR signaling pathway, diagnosis biomarker, macrophage polarization

Introduction

Chronic obstructive pulmonary disease (COPD) is a common chronic respiratory disorder characterized by persistent airflow limitation, which poses a significant global health burden.[1] Current therapeutic strategies offer only limited short-term relief and are ineffective in halting disease progression. As a result, researchers are actively exploring novel therapeutic approaches.[2] Although many potential therapies have shown limited efficacy, some have demonstrated improvements in lung function, pulmonary arterial hypertension, glucocorticoid sensitivity, and the frequency of acute exacerbations in patients with chronic obstructive pulmonary disease (COPD). These therapies include kinase inhibitors, cytokine and chemokine-targeted biological agents, small molecules, and peroxisome proliferator-activated receptor (PPAR) agonists.[2,3]

Received: 21 January 2025
Accepted: 29 June 2025
Published: 7 July 2025

PPARs, nuclear hormone receptors with antioxidant properties, are part of the nuclear receptor transcription factor superfamily and play a pivotal role in modulating target gene expression.[4] The activation state of PPARs significantly influences cell growth, differentiation, and apoptosis, and is implicated in various diseases, including cardiovascular diseases, diabetes, inflammation, and certain types of tumor growth.[5–7] The PPAR family consists of three subtypes: PPAR-α, PPAR-δ, and PPAR-γ. Dysregulation of PPAR family members, particularly PPAR-γ, has been associated with the onset of COPD.[8] Research indicates that PPAR-γ activation can suppress the production of pro-inflammatory cytokines, such as interleukin-6 (IL-6) and tumor necrosis factor-alpha (TNF-α), thereby reducing inflammation related to COPD.[8] Additionally, it promotes lung cell survival by inhibiting apoptotic pathway factors, including Bax and caspase activity, which may slow the progression of COPD.[9] In patients with COPD, PPAR-α expression is down-regulated; however, its activation can reduce the expression of inflammatory factors, such as interleukin-8 (IL-8) and monocyte chemoattractant protein-1 (MCP-1), while inducing antioxidant enzymes like superoxide dismutase (SOD), thus helping to combat oxidative stress-induced lung tissue damage.[10] Given the multifaceted roles of PPARs in COPD, they have emerged as potential therapeutic targets. Certain PPAR-γ agonists, such as thiazolidinediones, have demonstrated potential in alleviating emphysema[11] and reducing the risk of COPD exacerbation.[12]

Disruption of the immune microenvironment is one of the important mechanisms of COPD, and macrophages play a significant role in it. Alveolar macrophages (AMs) are at the forefront of the innate immune defense in the lungs and play a key role in cigarette smoke (CS)-induced pulmonary inflammation in COPD patients.[13,14] Macrophages have remarkable plasticity and can polarize into different phenotypes, namely pro-inflammatory M1 macrophages and anti-inflammatory M2 macrophages. Previous studies have shown that PPAR-γ can regulate the polarization of alveolar macrophages in COPD.[15,16] Although PPAR-γ exhibits potential regulatory effects on the polarization of alveolar macrophages (AMs) in COPD, current therapeutic approaches present certain limitations. Notably, synthetic PPAR agonists are associated with numerous off-target effects, and their efficacy is limited to specific groups of COPD patients,[3,9] primarily smokers.[17] Therefore, it is essential to conduct a comprehensive analysis of the genes involved in the PPAR pathway to clarify their roles in the pathogenesis and progression of COPD, as well as to explore alternative mechanisms for PPAR activation that could lead to new, more targeted treatments for COPD and other diseases related to chronic airway inflammation. Consequently, in this study, we conducted a comprehensive analysis of RNA sequencing (RNA-seq) and single-cell RNA sequencing (scRNA-seq) data from public databases to identify key genes in the peroxisome PPAR signaling pathway in patients with COPD. We ultimately dissected the potential mechanisms of these genes in the pathogenesis of COPD, including their impacts on the COPD immune microenvironment and cell-to-cell communication. Additionally, we partially validated these findings in population samples, providing new directions for the prevention and treatment of COPD.

Materials and Methods

Identification of Differentially Expressed Genes (DEGs) Between Individuals with COPD and Healthy Controls

In the GEO database (https://www.ncbi.nlm.nih.gov/geo/), three gene expression matrices associated with chronic obstructive pulmonary disease (COPD) were accessed: GSE57148 for sequencing data, and GSE76925 and GSE47460 for microarray data. The GSE57148 dataset comprised 98 subjects with COPD and 91 subjects with normal spirometry. The GSE76925 dataset included 111 COPD cases and 40 control smoker (all subjects were smokers). The GSE47460 dataset contained 144 COPD cases and 80 controls, and its clinical data were analyzed based on smoking status. The results are presented in Supplementary Table 2. All specimens involved were lung tissue. For the microarray data of GSE76925 and GSE47460, background correction was performed using backgroundCorrect in limma, normalization was carried out with the normalizeBetweenArrays function, and differential analysis was conducted using lmFit. For the sequencing data of GSE57148, after downloading the Count matrix, normalization was performed using the calcNormFactors TMM (Trimmed Mean of M-values) method in edgeR, and differential analysis was carried out with the glmQLFit and glmQLFTest functions. In the statistical analysis and assessment of differential expression, an empirical Bayes method was adopted to adjust the standard error of the estimated multiple changes for conducting

differential analysis, and genes with a p-value of less than 0.05 were identified as significantly differentially expressed genes.

Identification of PPAR Core Genes in Patients with COPD

For the differential genes of GSE57148, GSE76925, and GSE47460, a total of 551 shared differential genes were identified using the Venn intersection method. To conduct the functional enrichment analysis of these shared differential genes, we utilized the Gene Ontology (GO) annotation from the R package org.Hs.eg.db (version 3.1.0) and the KEGG pathway gene annotation accessed via the KEGG REST API (https://www.kegg.jp/kegg/rest/keggapi.html). The R package ClusterProfiler (version 3.14.3) was employed for the enrichment analysis. The minimum gene set size was established at 5, while the maximum was set at 5000, with P-values < 0.05 considered statistically significant. The PPAR pathway gene sets, BIOCARTA_PPARA_PATHWAY and KEGG_PPAR_SIGNALING_PATHWAY, were searched in the MSigDB database and intersected with the shared differential genes, resulting in the identification of 8 genes associated with the PPAR pathway.

PPAR Core Genes Correlation Analysis and Diagnostic Model Construction

Pearson correlation analysis was employed to assess the relationships among the PPAR hub genes. A positive correlation is indicated by a correlation coefficient approaching 1, while a negative correlation approaches −1. A p-value of less than 0.05 was established as the threshold for significant correlation. The diagnostic value of the PPAR core genes in chronic obstructive pulmonary disease (COPD) was evaluated using the receiver operating characteristic (ROC) curve, with a p-value of less than 0.05 considered statistically significant. A multi-parameter joint diagnostic model was constructed for the selected core genes using machine learning algorithms, specifically following the methodology outlined in the published literature regarding the construction and comparison of 113 models.[18]

Analysis of Immune Infiltration in COPD and Its Relationship with PPAR Core Genes

ImmucellAI (https://guolab.wchscu.cn/ImmuCellAI) was used to analyze immune cell infiltration in each sample. ImmucellAI is a tool designed to estimate the abundance of 24 immune cell types from gene expression datasets, including RNA-Seq and microarray data. This includes 18 T cell subtypes and 6 other immune cells: B cells, NK cells, monocytes, macrophages, neutrophils, and dendritic cells (DC). The Pearson correlation coefficient was employed to examine the relationship between PPAR core genes and infiltrating immune cells.

Analysis of scRNA-Seq

The scRNA-seq data from patients with COPD was obtained from the GSE136831, which included data from 18 COPD patients and 28 control lung tissue samples. The Python package Scanpy (version 1.9.3) was employed to process the data. Cells were filtered based on the following criteria: a minimum of 200 genes detected per cell, each gene expressed in at least three cells, less than 20% mitochondrial gene content, and a maximum of 4,000 unique molecular identifiers (UMIs) per cell. A total of 165,755 cells were retained for subsequent analysis. Subsequently, to identify the differential genes among various cell subpopulations, Scanpy compared one subpopulation of the sample with all other subpopulations. This comparison yielded a list of differential genes between the selected subpopulation and the remaining cell subpopulations. The CellMaker 2.0 database and the CellTypist package were utilized to annotate the cell subsets, while the R language, along with Seurat and ClusterGVis, was employed to analyze and visualize the annotated subsets of marker genes.

Preference Analysis of Cell Subsets

Based on the index used to characterize the meta-clusters in the published reference and STARTRAC analysis,[19] the distribution of the meta-clusters within the organization was examined. The odds ratio (OR) was calculated and used to indicate preference. An OR greater than 1.5 suggests a stronger inclination for distribution within the organization, while an OR less than 0.5 indicates a weaker tendency for distribution.

Cell-Cell Communication Analysis

The data were processed and analyzed using the CellChat package in R (version 4.1.3) to infer and interpret intercellular communication. CellChat (http://www.cellchat.org/) is a powerful tool that quantitatively infers, visualizes, and analyzes intercellular communication networks. It identifies key features of intercellular communication in single-cell RNA sequencing (scRNA-seq) datasets and predicts the potential functions of signaling pathways that have not been fully studied. In the analysis of cell interactions, the average expression value for each single-cell cluster or sample was calculated by determining the expression level relative to the total read length mapping of the same group of coding genes across all transcriptomes.

Proposed Temporal Sequence Analysis

Monocle2 (v2.12.0) was employed for single-cell pseudo-temporal analysis and cell trajectory sorting.[20] The input data required for Monocle2 analysis consisted of the TPM (Transcripts Per Million) matrix obtained after standardization. For cell annotation, we performed cell clustering analysis using Seurat software. Prior to the formal analysis, we preprocessed the data by estimating the size factor and dispersion to ensure the accuracy and reliability of subsequent analyses. Subsequently, we utilized the differential Gene Test function in Monocle2 to conduct differential gene detection. During this process, we set the p-value threshold at less than 0.05 and corrected for multiple tests using the Benjamini-Hochberg method as the screening criteria, thereby identifying genes that were dependent on pseudo-time. Based on the distinct expression patterns of these pseudo-time-dependent genes during cell development, we clustered them into three groups. The starting and ending points of the cell development trajectory timeline were determined based on known cell type-specific marker genes.

Recruitment Process and Participant Characteristics

Participants were enrolled at the Xinjiang Uygur Autonomous Region People's Hospital between July 1 and September 30. Eligible individuals, based on predefined inclusion and exclusion criteria, were sequentially sorted by hospital admission number and randomly selected using a computer-generated list, resulting in ten patients diagnosed with COPD. For each COPD patient, a health-matched individual was identified as a control subject, ensuring that both groups had comparable demographics, specifically matching gender and limiting the age difference to no more than five years. Statistical analysis confirmed that there were no significant differences in age or sex between the groups.

Inclusion Criteria for the COPD Group: 1. The diagnosis of COPD strictly adheres to the guidelines established in the 2024 Global Initiative for Chronic Obstructive Lung Disease (GOLD) report (goldcopd.org). 2. Patients categorized under GOLD Group E. 3. Patients without cognitive impairments. Exclusion Criteria for Participants: 1. The presence of alternative pulmonary conditions, such as asthma, bronchiectasis, pulmonary fibrosis, or any form of airway restriction; ongoing treatment for tuberculosis; or a history of tuberculosis within the past year. 2. A History of Lung Surgery. 3.Severe physical illnesses or psychiatric disorders. 4. Pregnancy or Breastfeeding. 5.Lack of consent to participate or inability to meet the study requirements.

Ethical Considerations and Informed Consent

Ethical approval for this study was granted by the Ethics Committee of the Xinjiang Uygur Autonomous Region People's Hospital (Ethics Committee Approval No: KY2024052256). Informed consent forms were signed by every participant, affirming their voluntary participation and understanding of the study's purpose and procedures. This recruitment strategy ensured a representative sample that met stringent eligibility standards, allowing for robust comparisons between COPD patients and matched controls, while upholding ethical research practices and safeguarding participant rights. This study complies with the Declaration of Helsinki.

Assessment of Gene Expression

Peripheral blood samples were collected from the subjects (control group = 10, COPD group = 10), and RNA was subsequently extracted to assess the expression of target genes in both groups using reverse transcription quantitative polymerase chain reaction. The clinical data of these subjects are presented in Supplementary Table 4. Total RNA extraction was performed using TRIZOL (Catalog No. 15596018, Invitrogen, USA). Complementary DNA (cDNA) synthesis was conducted with a reverse transcription kit (Catalog No. RR047A, TakaRa, Japan) at 42°C for 5 minutes, followed by 37°C for 15 minutes, and a final step at 85°C for 5 seconds, all executed on a MyCycler (Catalog No. RR820A, TakaRa, Japan). Quantitative PCR (qPCR) was performed on an ABI QuantStudio 5, which included an initial denaturation step at 95°C for 30 seconds, followed by 40 cycles of denaturation at 95°C for 15 seconds, and annealing and extension at 60°C for 34 seconds. Each sample was analyzed in triplicate technical replicates. The concentration of each transcript was normalized to ACTB, and mRNA levels were analyzed using the $2^{-\Delta\Delta CT}$ method. Comparisons were conducted using two-way ANOVA with GraphPad Prism software (Version 8.0, San Diego, CA). The primers used for quantitative PCR analysis are detailed in Supplementary Table 1.

Flow Cytometry

Peripheral blood samples (5 mL each) were collected from the subjects (control group = 16, COPD group = 17). The clinical data of these subjects are presented in Supplementary Table 3. Peripheral blood mononuclear cells (PBMCs) were isolated using density gradient centrifugation, washed, and counted to adjust the concentration. Fluorescently labeled antibodies specific to macrophage markers, along with isotype control antibodies, were selected. PBMC suspensions were placed in flow cytometry tubes, with the experimental group receiving a mixture of specific antibodies and the isotype control group receiving only isotype control antibodies. The tubes were incubated in the dark on ice. After multiple washes to remove unbound antibodies, the cells were resuspended. Finally, FlowJo and other software were utilized for analysis. Initially, a gate was established using forward scatter (FSC) and side scatter (SSC) to define monocytes, followed by the differentiation of M1 and M2 macrophage subtypes based on fluorescence labeling, and their proportions within the monocyte population were calculated.

Statistical Analysis

All measurements were performed independently, with each conducted at least in triplicate. The data were expressed as mean ± standard deviation (SD), and one-way ANOVA was utilized to evaluate differences between groups. A p-value of <0.05 or <0.01 was considered statistically significant.

Results

Overall Expression of Lung Tissue in Patients with COPD

After obtaining three lung tissue datasets related to COPD from GSE57148, GSE76925, and GSE47460, and eliminating any batch effects, we analyzed a total of 350 COPD patients and 220 healthy controls for expression profiling (Figure 1A–1C). An empirical Bayesian method was employed to adjust the standard error of the estimated fold change for conducting differential analysis, with a significance threshold set at $P < 0.05$ for identifying differentially expressed genes. Using a Venn diagram, we identified 551 differentially expressed genes that were common across all three groups (Figure 1D), and a heatmap illustrated the clustering of these genes (Figure 1E). Gene Ontology (GO) enrichment analysis indicated that these 551 genes are primarily associated with macromolecule localization, protein localization, transcription factor binding, and enzyme binding, among other functions (Figure 1F). Kyoto Encyclopedia of Genes and Genomes (KEGG) enrichment analysis revealed that these genes are predominantly enriched in the PI3K-Akt signaling pathway, GnRH signaling pathway, Hippo signaling pathway, Wnt signaling pathway, and PPAR signaling pathway (Figure 1G).

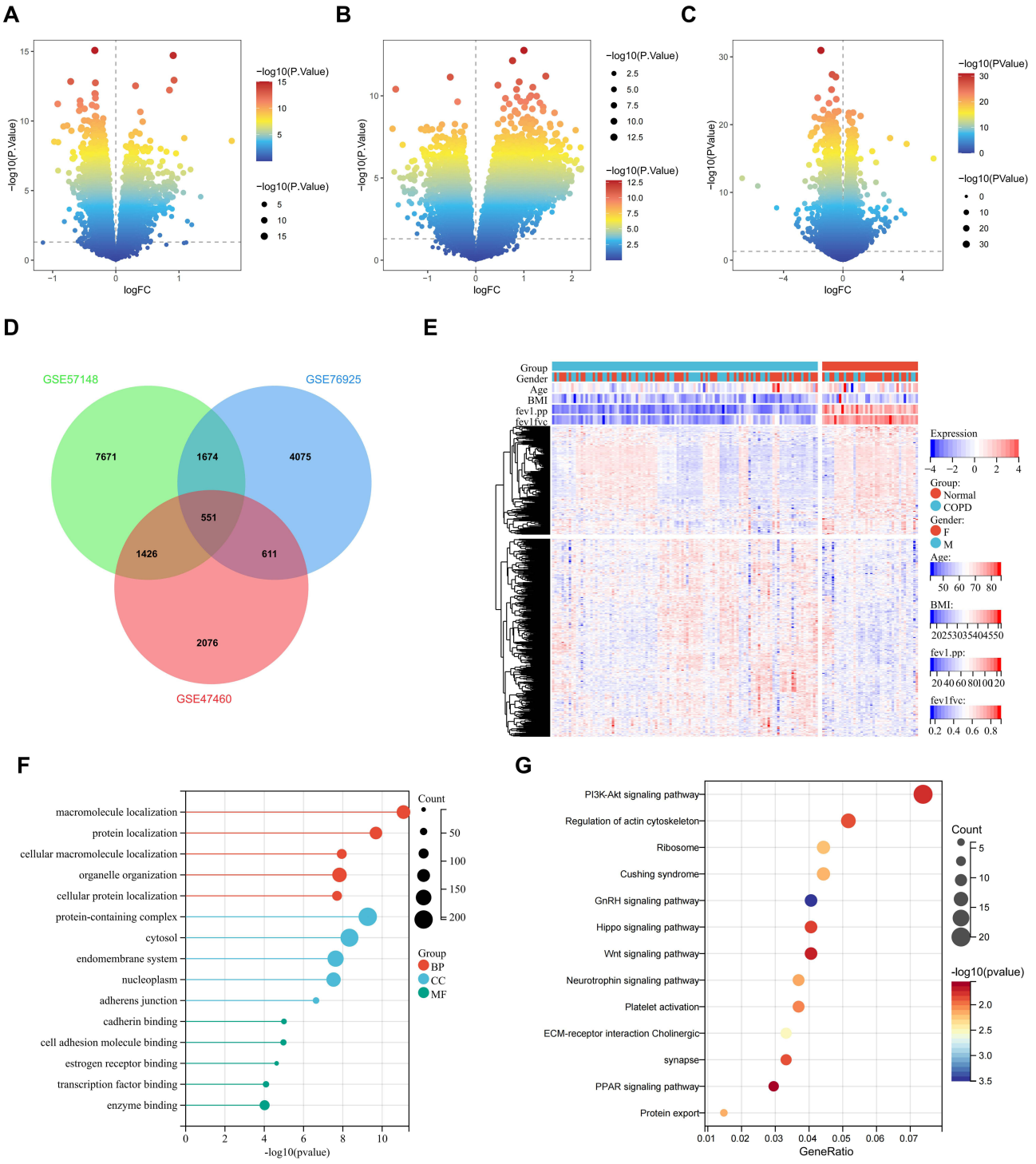

Figure 1 Overall expression of lung tissue in patients with COPD. (**A**) A volcano plot depicting the differentially expressed genes (DEGs) of GSE47460. (**B**) A volcano plot presenting the DEGs of GSE76925. (**C**) A volcano plot showing the DEGs of GSE57148. (**D**) A Venn diagram illustrating the intersection of DEGs in GSE57148, GSE76925, and GSE47460. A total of 551 shared DEGs were identified. (**E**) A heatmap displaying the expression distribution of the 551 shared genes. (**F**) A bubble plot shows the results of GO enrichment analysis of the shared DEGs. (**G**) A bubble plot shows the results of KEGG enrichment analysis of the shared DEGs.

Identification of PPAR Core Genes and Their Diagnostic Predictive Value in COPD

We identified eight core genes associated with the PPAR pathway by intersecting 551 common differentially expressed genes with the PPAR pathway. These genes are NCOR1, NCOA1, MED1, PPARGC1A, NRIP1, DUT, PLTP, and SLC27A5 (Figure 2A). Significant differences in the expression levels of these eight core genes were observed between

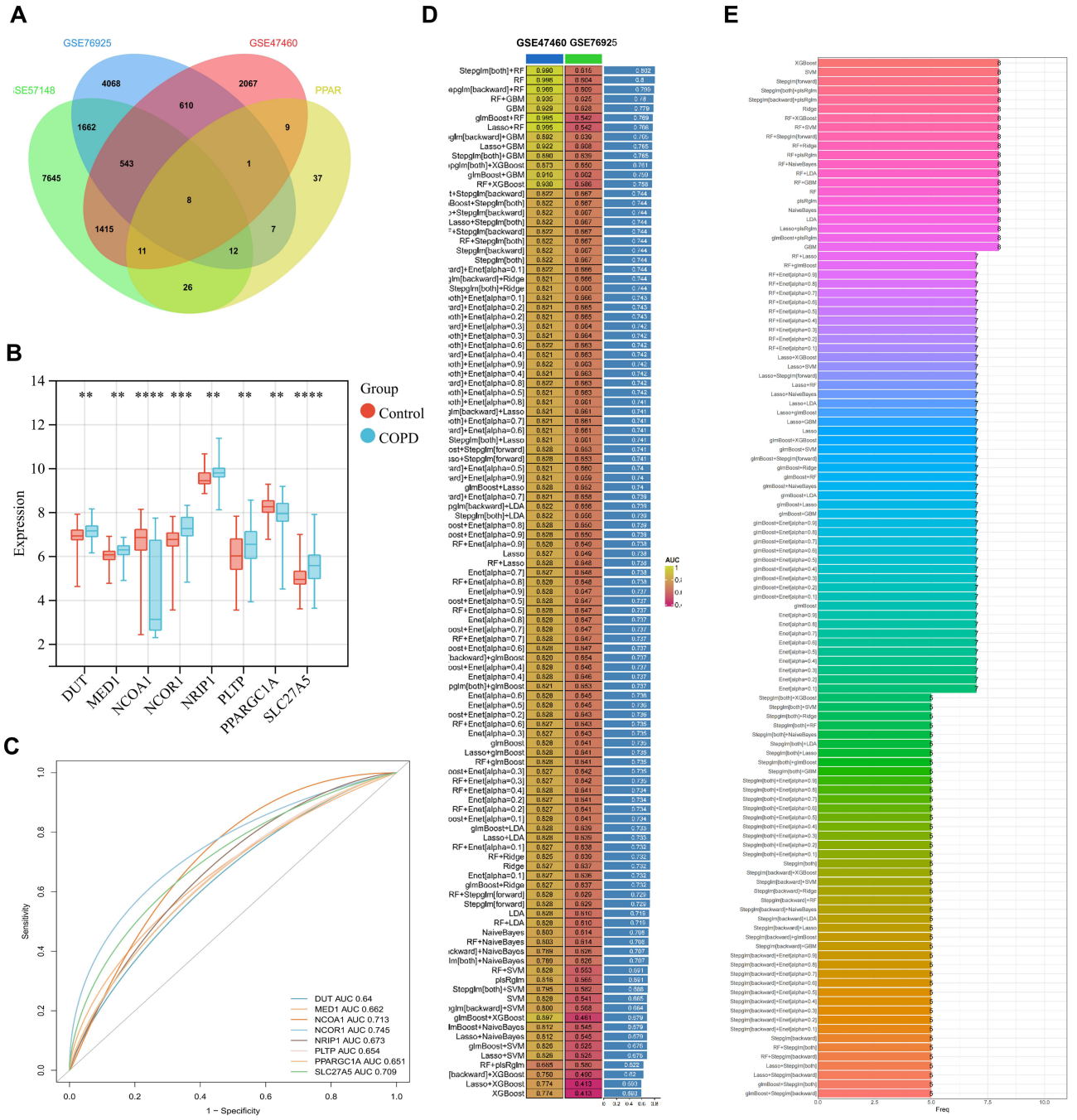

Figure 2 Identification and analysis of core genes in the PPAR pathway. (**A**) Using the Venn analysis method, the intersection of 551 common differentially expressed genes (DEGs) with BIOCARTA_PPARA_PATHWAY and KEGG_PPAR_SIGNALING_PATHWAY was calculated, and finally 8 PPAR core genes were obtained. (**B**) The expression levels of 8 PPAR genes in the chronic obstructive pulmonary disease (COPD) group and the control group. The relevant data were derived from GSE76925. *indicates $P < 0.01$, **indicates $P < 0.001$, and ****indicates $P < 0.0001$. (**C**) The receiver operating characteristic (ROC) curve was used to demonstrate the diagnostic value of 8 PPAR core genes in chronic obstructive pulmonary disease (COPD). The data were sourced from GSE76925. (**D**) For the 8 PPAR core genes, 113 model construction and comparison tasks were carried out. In the result presentation, the 113 algorithms are listed on the leftmost side; the second column shows the training set (data from GSE47460); the third column presents the validation set (data from GSE76925); and the rightmost side gives the area under the curve (AUC) of each model. (**E**) This figure shows the number of core genes included in 113 algorithm combination patterns.

the COPD group and the control group. Specifically, NCOA1 and PPARGC1A were downregulated in the lung tissue of COPD patients, while NCOR1, MED1, NRIP1, DUT, PLTP, and SLC27A5 were upregulated. The data were sourced from GSE76925 (Figure 2B). Correlation analysis revealed that NCOA1 was negatively correlated with NCOR1, SLC27A5, and PLTP, whereas NCOR1 exhibited a positive correlation with MED1, DUT, NRIP1, and PLTP (Supplementary Figure 1A). We evaluated the discriminatory potential of these genes for distinguishing COPD patients

https://doi.org/10.2147/COPD.S518592

from healthy individuals using Receiver Operating Characteristic (ROC) analysis. The results indicated that NCOA1, NCOR1, and SLC27A5 demonstrated significant discriminatory ability, with an Area Under the Curve (AUC) greater than 0.7, based on data from GSE76925 (Figure 2C). Using GSE47460 as the training set and GSE76925 as the validation set, and referencing relevant literature,[18] we constructed diagnostic prediction models for the eight core genes. The optimal combination model included PPARGC1A, MED1, PLTP, NRIP1, and SLC27A5 (Stepglm[both] + RF), achieving an AUC of 0.802 (Figure 2D and E).

The Influence of Smoking on the Core Genes of the PPAR Pathway

Given that smoking is a major contributing factor to COPD, it is of great significance to deeply explore whether smoking has a specific impact on the regulation of the PPAR pathway. In this study, we conducted a detailed analysis of the GSE47460 dataset, focusing on the expression of key PPAR genes in smoking and non-smoking patients (Supplementary Figure 1). The results showed that the selected 8 genes exhibited significant expression differences between the smoking control group and the smoking COPD patients, as well as between the smoking control group and the non-smoking COPD patients (Supplementary Figure 2). These findings strongly suggest that the expression of PPAR pathway genes is significantly affected by smoking. Such differences in gene expression likely indicate that smoking interferes with the normal regulation of the PPAR pathway through a unique molecular mechanism, thereby playing a promoting role in the pathogenesis of COPD.

The PPAR Core Gene Is Associated with the Immunological Characteristics of Patients with COPD

We compared the levels of immune cell infiltration between patients with COPD and healthy controls. The results indicated a phenomenon of immune dysregulation in COPD patients (Supplementary Figure 1B). Genes associated with the PPAR pathway showed significant correlations with various immune cells (Figure 3A). Specifically, NCOA1 exhibited a negative correlation with macrophages, natural killer T (NKT) cells, and effector memory cells, while it was positively correlated with neutrophils and monocytes. Conversely, NCOR1 was positively correlated with macrophages, natural killer (NK) cells, NKT cells, and effector memory cells. NRIP1 demonstrated positive correlations with neutrophils, macrophages, B cells, monocytes, and T cells. Notably, PPARGC1A was significantly negatively correlated with most immune cell infiltration levels, while SLC27A5 showed a positive correlation with NKT cells. Additionally, PLPT was positively correlated with T cells and B cells. The abnormal expression of these genes may contribute to the immune dysregulation observed in COPD. To further investigate the role of PPAR in immune cells in COPD, we analyzed the scRNA seq data from GSE136831 for COPD patients. A total of 165,755 cells were included in the subsequent analysis (Figure 3B). We present the distribution of cell clusters, with cells in the same cluster represented by the same color (Figure 3C). Utilizing classical marker genes, we categorized the cells into 14 types (Figure 3D and E).

Analyze Immune Cells in Patients with COPD Using scRNA-Seq Data

Compared to the control group, the immune cell infiltration status in the COPD group exhibited notable differences (Figure 4A). Specifically, regarding cell proportions, the levels of M1 and M2 macrophages, as well as monocytes, were significantly lower in the COPD group than in the control group. Conversely, the proportions of T cells, B cells, and NK cells were higher in the COPD group compared to the control group (Figure 4B and C). Further analysis of macrophages revealed that M2 macrophages predominated in both the control and COPD groups (Figure 4D). In terms of PPAR pathway genes, NCOR1 and NCOA1 demonstrated significant accumulation in macrophages and monocytes, while the expression levels of PPARGC1A and SLC27A5 were relatively low in macrophages (Figure 4E).

The COPD Group Exhibits Altered Intercellular Communication When Compared to the Control Group

We conducted an analysis of intercellular communication in both the COPD group and the control group. An overview of all cell populations is presented in Supplementary Figure 3. Additionally, significant differences in intercellular communication were observed between the COPD group and the control group (Figure 5A and B). In the COPD group, there

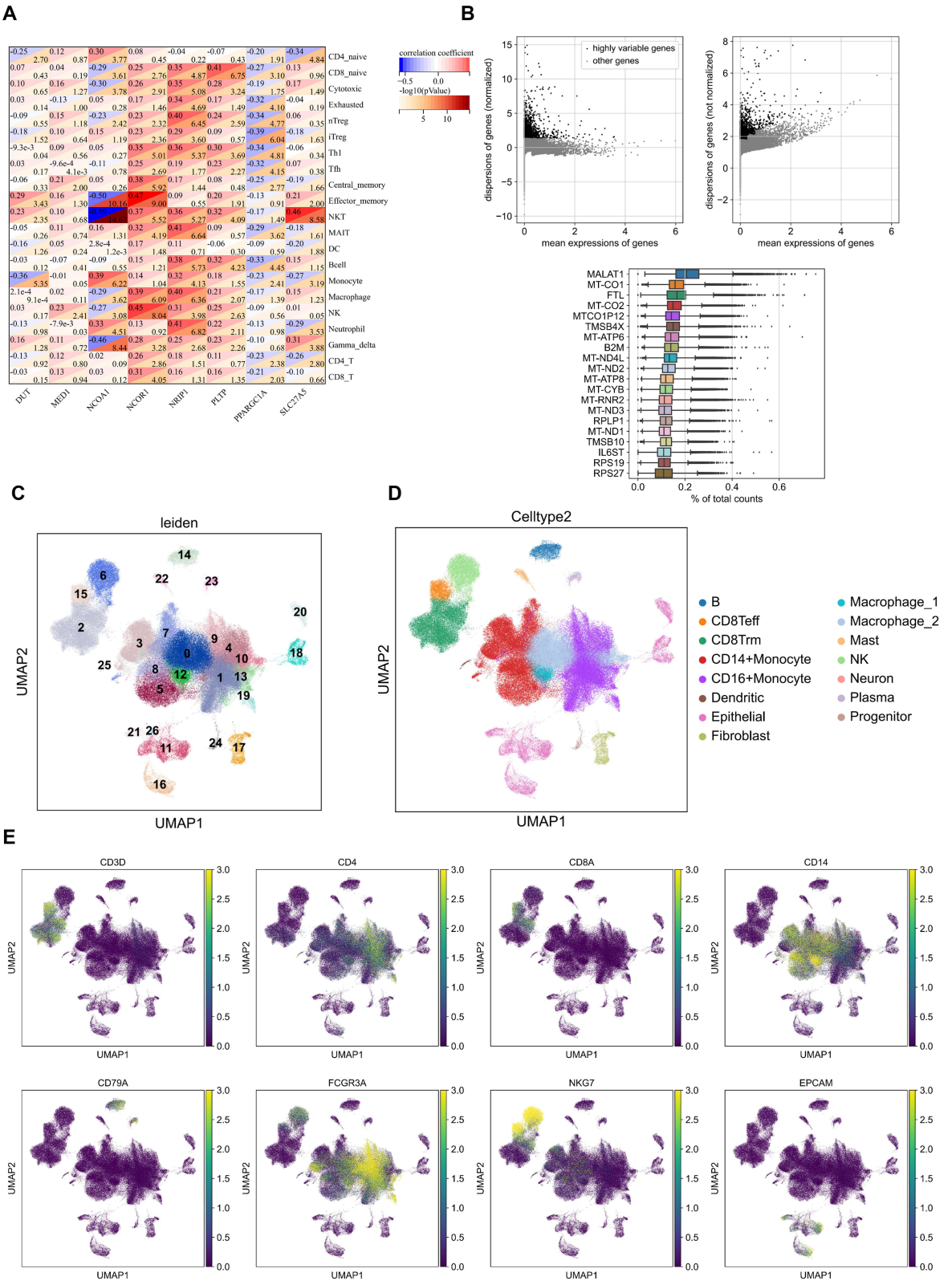

Figure 3 Analysis of immune cells in COPD patients using scRNA-seq. (**A**) Correlation analysis between PPAR genes and immune cells. The data for the correlation analysis among PPAR genes were derived from GSE76925. (**B**) Screening of highly variable genes in single-cell sequencing. (**C**) Uniform Manifold Approximation and Projection (UMAP) plot for cell clustering analysis, colored by clusters. (**D**) Uniform Manifold Approximation and Projection (UMAP) plot showing the annotation and color codes for cell types. (**E**) The UMAP plot showing the expression levels of different cell markers in cell subsets.

https://doi.org/10.2147/COPD.S518592

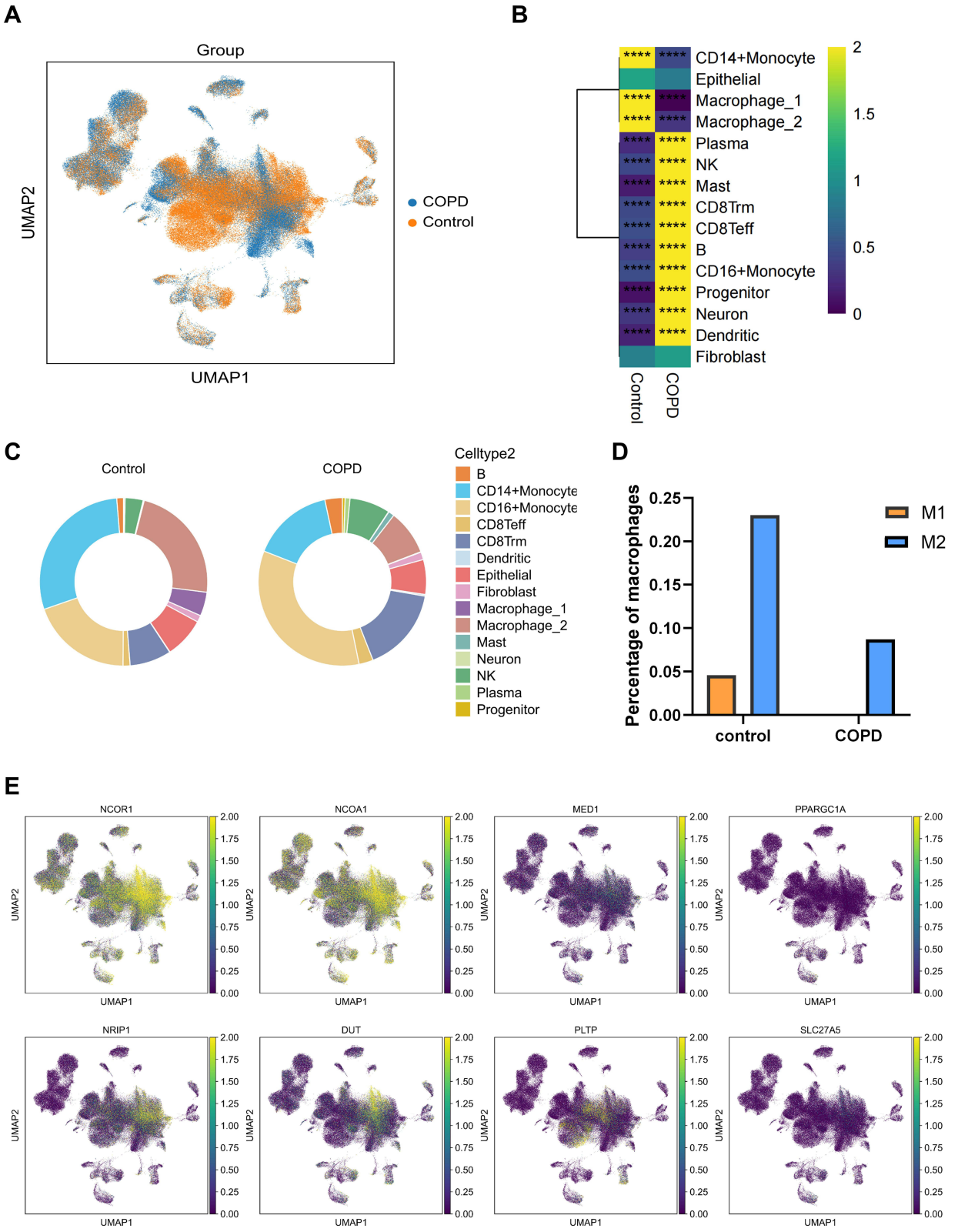

Figure 4 Analysis of immune cells in COPD and control groups. (**A**) The UMAP plot shows the infiltration of immune cells in the COPD and control groups. (**B**) The tissue preferences of each immune cell cluster are presented. The odds ratio (OR) is calculated to represent the preference. When OR > 1.5, it indicates that the cells tend to be distributed in this tissue; when OR < 0.5, it means that the cells are less likely to be distributed in this tissue. *P < 0.01, **P < 0.001, ****P < 0.0001. (**C**) The pie chart shows the percentages of various cell types in the COPD and control groups. (**D**) The bar chart shows the proportions of M1 and M2 macrophages in the COPD and control groups. (**E**) The UMAP plot shows the distribution of PPAR core genes in cells.

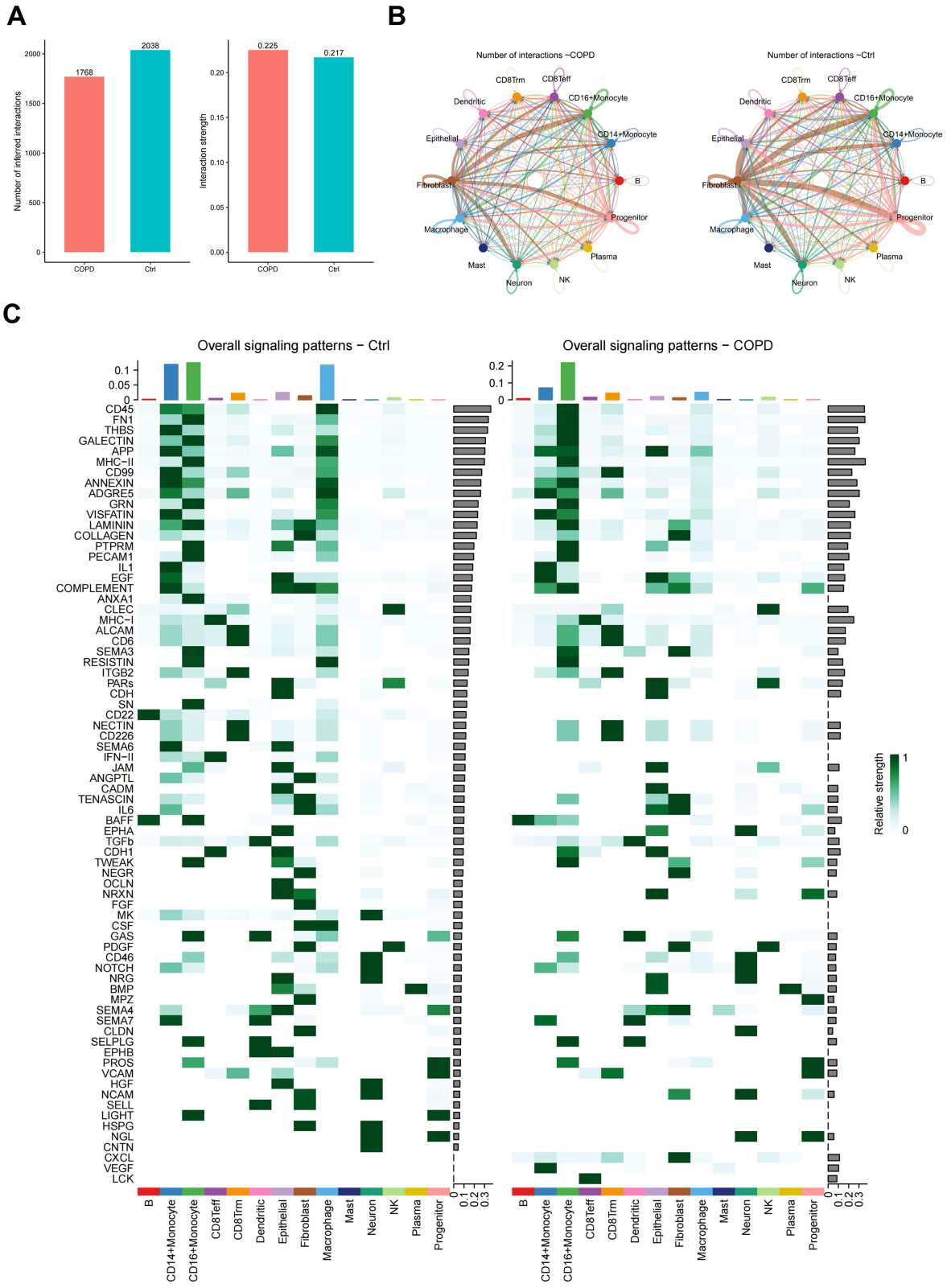

Figure 5 Analysis of intercellular communication. (**A**) A holistic view of all cell populations: The quantity and intensity of overall intercellular communication under COPD and healthy conditions were compared. (**B**) The chord diagram presents a network graph comparing the number of cell interactions in the COPD group and the control group. Each color represents a different cell type, the arrows indicate the direction, and the thickness of the lines represents the number of interactions. (**C**) The heatmap shows the signal intensities of signaling pathways within specific cell populations in the COPD group and the control group. The horizontal axis represents cell types, and the vertical axis represents signaling pathways.

https://doi.org/10.2147/COPD.S518592

was a notable reduction in the number of communications between macrophages and CD14 monocytes, while intercellular communication involving CD16 monocytes increased (Figure 5C). Further analysis of the genes influencing macrophage communication revealed that genes associated with macrophage activation and polarization in the COPD group (such as CD45,[9] APP,[21] ANNEXIN,[22,23] ADGRE5,[24] and CSF[25]) were significantly downregulated compared to the control group (Figure 5C).

Pseudotemporal Analysis of Macrophages in Patients with COPD

We identified macrophages within the cell population by screening for characteristic genes and demonstrated their developmental trajectory in pseudo-time (Figure 6A and B). Based on the expression patterns, macrophages were

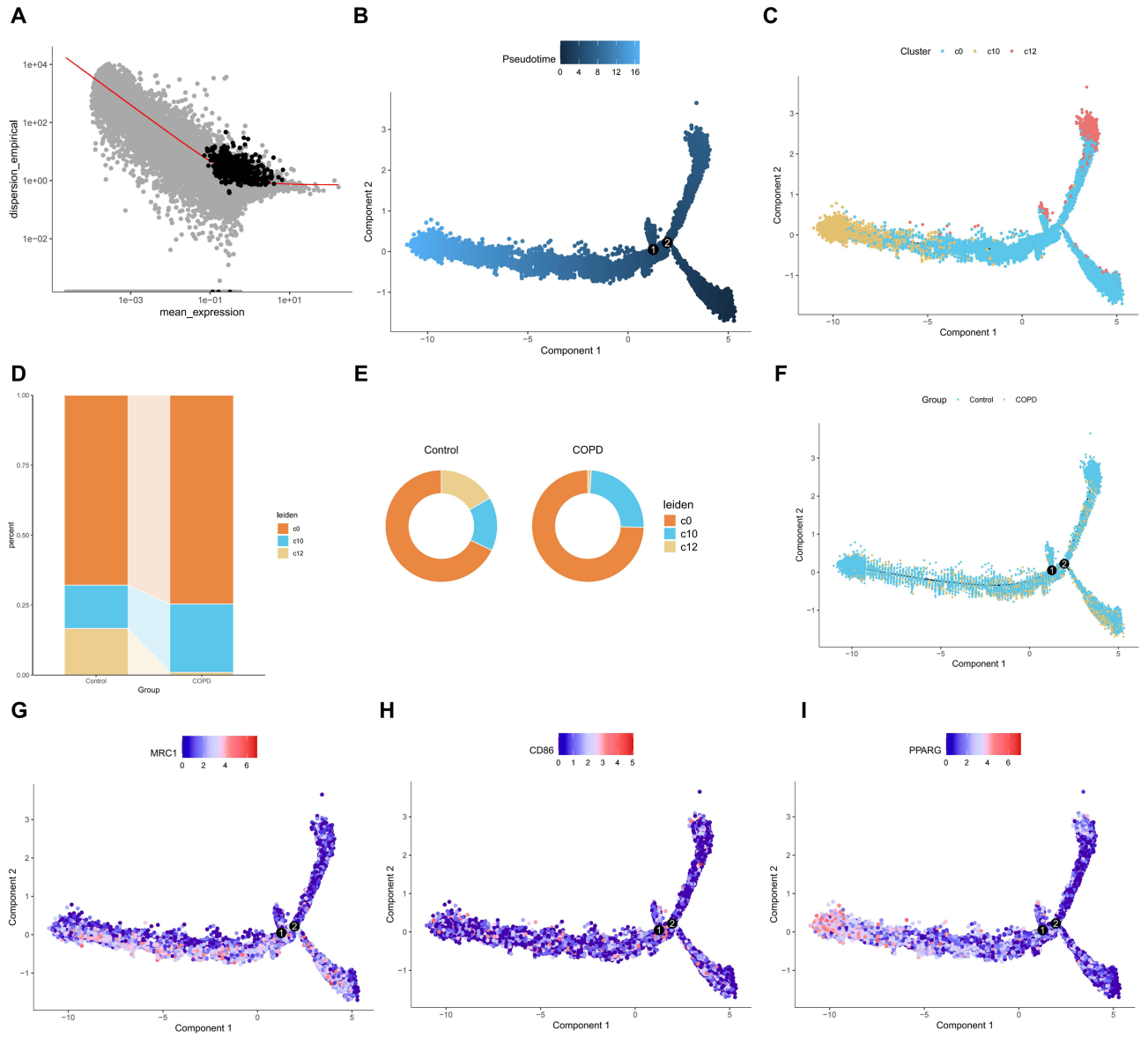

Figure 6 Pseudotemporal analysis of macrophages. (**A**) Macrophages were screened based on marker genes. (**B**) The developmental trajectory of macrophages. The start and end of the timeline are determined by known marker genes. (**C**) According to different expression patterns, pseudotime-dependent genes were clustered into three clusters, namely C0, C10, and C12. These three clusters correspond to the cell clusters in Figure 3D. Among them, C0 is colored blue, C10 is yellow, and C12 is red. The distribution of these three clusters of cells along the developmental trajectory is shown. (**D**) The bar chart shows the distribution of the three clusters C0, C10, and C12 in the control group and the COPD group. (**E**) The pie chart shows the distribution of the three clusters C0, C10, and C12 in the control group and the COPD group. (**F**) The distribution of the three clusters C0, C10, and C12 during the time period inferred by the trajectory. (**G**) The expression of M2 macrophage marker genes along the pseudotime line. (**H**) The expression of M1 macrophage marker genes along the pseudotime line. (**I**) The expression of PPARγ along the pseudotime line.

classified into three clusters: C0, C10, and C12 (Figure 6C). In the COPD group, the proportion of the C12 cell cluster was significantly decreased, while the proportion of the C10 cell cluster was significantly increased (Figure 6D and E). MRC1 serves as a marker gene for M2 macrophages and is primarily expressed in the C0 and C10 cell clusters (Figure 6G). Conversely, the marker gene for M1 macrophages, CD86, is uniformly expressed across the C0, C10, and C12 cell clusters (Figure 6H). As illustrated in Figure 6C, the C0 and C10 cell clusters predominantly exhibit M2 characteristics, while the C12 cell cluster is more aligned with M1 characteristics. Additionally, the C10 cell cluster may represent an intermediate transitional state or possess bidirectional traits. The developmental trajectory indicates that macrophages in COPD tend to polarize towards the M2 phenotype (Figure 6F). The accumulation of PPARγ in both C10 and C0 cell clusters suggests that PPARγ may be associated with the M2 polarization of macrophages in COPD (Figure 6I).

PPAR Pathway Genes May Play a Role in Regulating the Polarization of Macrophages in Patients with COPD

Upon reviewing the aforementioned findings and consulting relevant literature, we focused on validating the expression of genes associated with PPARγ and macrophages. The qPCR results demonstrated that NCOR1, NRIP1, and SLC27A5 were upregulated in patients with COPD, whereas NCOA1, PGC1A, and PPARγ were downregulated (Figure 7A). These findings were consistent with our sequencing data. Additionally, we measured the number of macrophages in the peripheral blood of COPD patients. The flow cytometry results demonstrated indicated the number of M2 macrophages in patients with COPD was higher compared to that in the control group (Figure 7B). The aforementioned findings suggest a polarization disorder of M1 and M2 macrophages in COPD, characterized by a predominant shift towards the M2 phenotype. PPARs are likely to play a critical role as key pathways and molecules driving M2 polarization, which may subsequently influence immune cell infiltration levels and contribute to the progression of COPD.

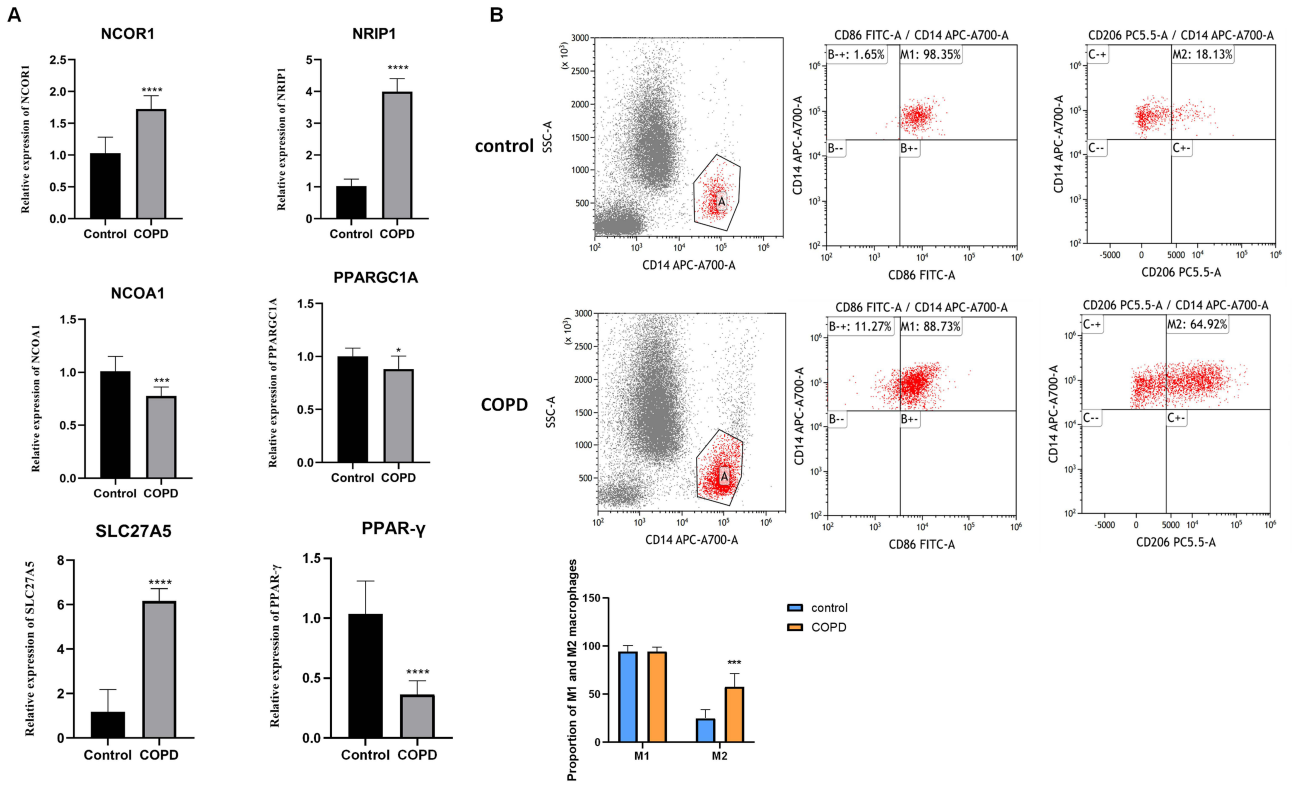

Figure 7 Expression of PPAR core genes and distribution of macrophages in patients with COPD. (**A**) RT-qPCR was used to detect the expression of PPAR core genes in healthy controls and patients with COPD. *$P < 0.01$, **$P < 0.001$, ****$P < 0.0001$. (**B**) Flow cytometry was employed to measure the proportion of macrophages in the peripheral blood of healthy controls and patients with COPD.

https://doi.org/10.2147/COPD.S518592

Discussion

PPARs (Peroxisome Proliferator-Activated Receptors), particularly PPAR-γ, play a central role in the onset and progression of COPD due to their extensive involvement in regulating inflammation, cell survival, oxidative stress, and metabolic balance.[9,26,27] Although synthetic PPAR-γ agonists have shown potential in counteracting COPD, concerns remain regarding their efficacy and side effects in clinical applications. The dual effects of these drugs, balancing efficacy and adverse reactions, primarily arise from the complex drug-target dynamics, with off-target effects being widespread. This highlights the challenges in drug design.[28] Therefore, this study aims to explore key molecules within the PPAR signaling pathway in the context of COPD and to identify biomarkers closely associated with the disease.

Smoking is one of the significant inducements of COPD. Research has found that smoking has a multi-dimensional and significant impact on the PPAR pathway. Harmful substances in cigarettes can interfere with the normal activation and signal transduction process of PPARγ. Perinatal injection of nicotine can also cause intergenerational transmission of PPARγ-dependent asthma.[29] Meanwhile, smoking-mediated PPARγ gene polymorphism increases the risk of cardiovascular disease (CVD) in smokers.[30] In terms of addiction, PPAR is located in addiction-related brain regions. Animal experiments have shown that its agonists can reduce the characteristics of addictive drugs, but the results of human studies are inconsistent. For instance, PPARα agonists have no effect on nicotine outcomes, while PPARγ agonists are only effective in reducing drug craving in some studies.[31] Additionally, in chronic airway diseases, interfering with PPAR can regulate cigarette smoke-induced inflammation. For example, erythromycin and bexarotene respectively inhibit or improve related lung inflammation through specific signaling pathways.[14,32] In our study, we analyzed the expression of key PPAR genes in both smoking and non-smoking patients. The results showed that the selected 8 genes were differentially expressed in both the smoking control group and the smoking COPD patients, as well as between the smoking control group and the non-smoking COPD patients. These findings may suggest that smoking interferes with the normal regulation of the PPAR pathway through a unique molecular mechanism, thereby contributing to the pathogenesis of COPD. The gene expression differences between the smoking control group and the smoking COPD patients might reflect the dynamic changes in the PPAR pathway due to continuous exposure to tobacco harmful substances during disease progression, which may gradually drive the condition from a relatively healthy state to COPD. The gene expression differences between the smoking control group and the non-smoking COPD patients highlight the specific role of smoking as an exogenous stimulus in altering the expression of PPAR pathway genes, distinct from other non-smoking factors that may cause COPD. Further studies could focus on the specific functions of these differentially expressed genes, exploring how they interact and their association with the pathological features of COPD.

Through a combination of screening and literature review, we have identified five candidate genes: NCOR1, NRIP1, NCOA1, PARGC1A, and SLC27A5. The activation of PPARs is initiated by the binding of ligands to the hydrophobic pocket of the receptor, which induces a conformational change in the receptor. This process leads to the dissociation of NCoR/SMRT and histone deacetylase (HDAC), followed by the recruitment of coactivators such as PARGC1A, SRC-1, and histone acetyltransferase (HAT). These factors collectively promote chromatin remodeling, facilitating the binding of RNA polymerase II and subsequently initiating the transcription of target genes.[33] Cofactors play a crucial role in PPAR-γ function, with the strength of ligand effects varying across different cell types. This variation is reflected in the distinct activity of partial or full agonists, which is closely linked to the distribution of cofactor profiles.[34] Even within the same cell type, a ligand may act as a full agonist in one cofactor (eg, NCoR) while serving as a partial agonist in others (eg, PARGC1A and DRIP/TRAP220).[35]

The selected genes—NCOR1, NRIP1, NCOA1, PARGC1A, and SLC27A5—form a complex regulatory network with PPAR-γ. NCOR1, functioning as a corepressor of PPAR-γ, plays a crucial role in maintaining immune-metabolic homeostasis. Research has demonstrated that stabilizing the interaction between NCOR1 and PPAR-γ inhibits the expression of target genes in both mouse and human macrophages, thereby influencing immune metabolism.[36] Furthermore, NCOR1 is essential for immune tolerance; its deletion increases the expression of IL-10, IL-27, and SOCS3, thereby promoting an immune-tolerant state in dendritic cells (DCs) and reprogramming their metabolism to elicit a specific immune response.[37] NRIP1 (RIP140), another ligand-dependent corepressor, plays a dual role in regulating metabolism and inflammation by modulating PPAR signaling.[38–40] NCOA1[41,42] and PARGC1A[43] are

coactivators of PPAR-γ, with PARGC1A potentially mitigating inflammation and oxidative stress in COPD.[44,45] Notably, NCOR1 and NRIP1 are upregulated in COPD, whereas the expression of PARGC1A and NCOA1 is significantly downregulated. This contrasting expression pattern underscores their potential as biomarkers and may provide new opportunities for early diagnosis and prognostic monitoring of COPD. MED1 is primarily associated with PPAR-α,[46] while SLC27A5 may be a target of PPAR, although its precise role remains unclear.[47]

Single-cell sequencing results revealed an immune imbalance in the lung tissues of COPD patients, particularly in the proportions of immune cells and intercellular communication, which significantly differed from those in healthy controls. Macrophages play a core role in this immune dysregulation process, and their immune regulation and tissue repair functions in COPD are crucial. The polarization state of macrophages directly affects the progression of the disease.[27,48] Single-cell sequencing results indicate that M2-type macrophages are dominant in the lung tissue of COPD patients, and pseudo-time analysis further supports this finding. To verify the results of single-cell sequencing at the overall level, we detected the proportion of macrophages in the peripheral blood of COPD patients and healthy controls. The results showed that the proportion of M2 macrophages in COPD patients was significantly higher than that in the control group ($P < 0.05$), indicating that the polarization tendency of macrophages in COPD patients shifts towards the M2 type. There remains controversy regarding the status of macrophages in COPD. Our research findings are consistent with those of Byers DE.[49] They compared non-COPD patients, IV-stage COPD lung transplant recipients (n = 16), non-transplantable donor lung tissues (n = 7), and resected lung tissues from patients with GOLD stages I to IV (n = 55), and found that M2-type macrophages were activated in COPD lung tissues. Consistent with this, Cornwell[50] also reported that there was an abnormal population of M2-like monocytes in the blood of patients with severe COPD.

Macrophage reprogramming is strictly regulated by the PPAR signaling. Among them, PPAR-γ plays a crucial role in the pathological process of COPD. Previous studies have reported that PPAR-γ can modulate the polarization of alveolar macrophages in COPD[15,16] and delay their aging process.[26,27] Our pseudotime analysis results further revealed that PPAR-γ is highly expressed in cell clusters that tend to differentiate into M2 macrophages. In the regulation of macrophage polarization, multiple key genes play important roles. First, NCOR1 and NRIP1 have a significant impact on the polarization direction of macrophages. Specifically, the upregulation of NCOR1 and NRIP1 promotes macrophage polarization towards the M1 type. Conversely, when NCOR1 is deficient, the number of M2 macrophages increases, thereby exacerbating allergic airway inflammation.[51] NCOR1 also influences immune responses by regulating glucose metabolism reprogramming (GMR) in macrophages.[52,53] Regarding NRIP1, its overexpression in macrophages drives M1 polarization and cell expansion during the inflammatory response. On the contrary, a decrease in NRIP1 expression reduces the number of M1 macrophages and increases the number of M2 macrophages.[54] In addition to the above genes, PARGC1A and NCOA1 are also of great significance in the regulation of macrophage differentiation. PARGC1A, as a key factor in maintaining mitochondrial homeostasis in macrophages, its activation can promote mitochondrial biogenesis in monocyte - derived macrophages.[55] However, this process promotes the development of pulmonary fibrosis.[56] NCOA1 enhances macrophage recruitment and migration by targeting M-CSF1, and its silencing reduces CSF1 expression, thereby decreasing macrophage recruitment and breast cancer cell metastasis.[57] Single - cell sequencing data provides a new perspective for understanding the roles of these genes. The data shows that NCOR1, NRIP1, and NCOA1 are highly enriched in macrophages and monocytes, while the expression levels of PARGC1A and SLC27A5 in macrophages are relatively low. Based on the above research results, these core genes of the PPARs pathway are likely to finely regulate macrophage polarization and function by modulating the activity of PPAR-γ, ultimately affecting the progression of COPD. The increase in M2 macrophage numbers in patients with chronic obstructive pulmonary disease (COPD) may be closely related to the decline in immune function. The cells of COPD patients have characteristics such as decreased antigen processing ability, abnormal inflammatory response, and loss of immune response regulation function. As M2 macrophages mainly exert anti-inflammatory effects, this feature in COPD patients may lead to ineffective immunity. The weakening of immune function further increases the risk of infection for patients and maintains a persistent chronic inflammatory state in the lungs.[58,59] In addition, since M2 macrophages are believed to be associated with tissue repair and remodeling as well as tumor promotion, the increase in the M2/M1 phenotype ratio may play an important role in the remodeling of small airways in COPD.[60]

Conclusion

Given the unique regulatory role of PPARγ in COPD, along with the profound impact of key genes such as NCOR1, NRIP1, NCOA1, and PARGC1A on PPARγ activity, these genes hold significant potential as therapeutic targets. By targeting these genes, researchers can develop more precise intervention strategies aimed at correcting macrophage polarization dysregulation, alleviating inflammation, and promoting tissue repair. At present, our research is based solely on RNA sequencing results from public databases. Further validation experiments using animal models or samples from patients' bodies are still needed in the future. This study offers new insights into the immune dysfunction underlying COPD and paves the way for innovative therapeutic approaches, heralding the era of personalized medicine.

Data Sharing Statement

All data generated or analyzed during this study are publicly available. They can be obtained from the corresponding author upon reasonable request. The data include raw experimental data, processed data, and relevant metadata.

Funding

The authors appreciate the support from the Tianchi Talent Program (TCYCQNBS) and Tianshan Talents Program (Project No. TSYC202301A029) of the Xinjiang Uygur Autonomous Region.

Disclosure

The authors declare that they have no conflicts of interest in this work.

References

1. Halpin DMG. Mortality of patients with COPD. *Expert Rev Respir Med*. 2024;18:381–395. doi:10.1080/17476348.2024.2375416
2. Uwagboe I, Adcock IM, Lo Bello F, Caramori G, Mumby S. New drugs under development for COPD. *Minerva Med*. 2022;113:471–496. doi:10.23736/s0026-4806.22.08024-7
3. Lakshmi SP, Reddy AT, Reddy RC. Emerging pharmaceutical therapies for COPD. *Int J Chron Obstruct Pulmon Dis*. 2017;12:2141–2156. doi:10.2147/copd.S121416
4. Vázquez-Carrera M, Wahli W. PPARs as key transcription regulators at the crossroads of metabolism and inflammation. *Int J Mol Sci*. 2024;25:4467. doi:10.3390/ijms25084467
5. Christofides A, Konstantinidou E, Jani C, Boussiotis VA. The role of peroxisome proliferator-activated receptors (PPAR) in immune responses. *Metabolism*. 2021;114:154338. doi:10.1016/j.metabol.2020.154338
6. Lange NF, Graf V, Caussy C, Dufour JF. PPAR-targeted therapies in the treatment of non-alcoholic fatty liver disease in diabetic patients. *Int J Mol Sci*. 2022;23:4305. doi:10.3390/ijms23084305
7. Basilotta R, Lanza M, Casili G, et al. Potential therapeutic effects of PPAR ligands in glioblastoma. *Cells*. 2022;11. doi:10.3390/cells11040621
8. Liu D, Liu Z, Ma X, et al. Shengmai Powder regulates alveolar macrophage PPAR-γ and improves the chronic inflammatory state of chronic obstructive pulmonary disease. *Allergol Immunopathol*. 2024;52:73–79. doi:10.15586/aei.v52i5.1135
9. Li Q, Zhang H, Yan X, et al. Up-regulation of PPAR-γ involved in the therapeutic effect of icariin on cigarette smoke-induced inflammation. *Pulm Pharmacol Ther*. 2023;79:102197. doi:10.1016/j.pupt.2023.102197
10. Li H, Pei W, Wang Y, et al. Mechanism of action of the plateau-adapted gene PPARA in COPD. *Front Biosci*. 2024;29:68. doi:10.31083/j.fbl2902068
11. Shan M, You R, Yuan X, et al. Agonistic induction of PPARγ reverses cigarette smoke-induced emphysema. *J Clin Invest*. 2014;124:1371–1381. doi:10.1172/jci70587
12. Rinne ST, Feemster L, Collins B, et al. Thiazolidinediones are associated with a reduced risk of COPD exacerbations. *Int J Chron Obstruct Pulmon Dis*. 2015;10:1591–1597. doi:10.2147/copd.S82643
13. Kapellos TS, Bassler K, Aschenbrenner AC, Fujii W, Schultze JL. Dysregulated functions of lung macrophage populations in COPD. *J Immunol Res*. 2018;2349045. doi:10.1155/2018/2349045.
14. Feng H, Li Z, Zheng R. Bexarotene ameliorated the pulmonary inflammation and M1 polarization of alveolar macrophages induced by cigarette smoke via PPARγ/HO-1. *Respir Res*. 2024;25:431. doi:10.1186/s12931-024-03064-x
15. Yan S, Ding J, Wang Z, et al. CTRP6 regulates M1 macrophage polarization via the PPAR-γ/NF-κB pathway and reprogramming glycolysis in recurrent spontaneous abortion. *Int Immunopharmacol*. 2023;124:110840. doi:10.1016/j.intimp.2023.110840
16. Tu Y, Liu J, Kong D, et al. Irisin drives macrophage anti-inflammatory differentiation via JAK2-STAT6-dependent activation of PPARγ and Nrf2 signaling. *Free Radic Biol Med*. 2023;201:98–110. doi:10.1016/j.freeradbiomed.2023.03.014
17. Feng H, Yin Y, Zheng R, Kang J. Rosiglitazone ameliorated airway inflammation induced by cigarette smoke via inhibiting the M1 macrophage polarization by activating PPARγ and RXRα. *Int Immunopharmacol*. 2021;97:107809. doi:10.1016/j.intimp.2021.107809
18. Liu Z, Liu L, Weng S, et al. Machine learning-based integration develops an immune-derived lncRNA signature for improving outcomes in colorectal cancer. *Nat Commun*. 2022;13:816. doi:10.1038/s41467-022-28421-6
19. Zheng L, Qin S, Si W, et al. Pan-cancer single-cell landscape of tumor-infiltrating T cells. *Science*. 2021;374:abe6474. doi:10.1126/science.abe6474

20. Trapnell C, Cacchiarelli D, Grimsby J, et al. The dynamics and regulators of cell fate decisions are revealed by pseudotemporal ordering of single cells. *Nat Biotechnol*. 2014;32:381–386. doi:10.1038/nbt.2859
21. Taylor X, Clark IM, Fitzgerald GJ, et al. Amyloid-β (Aβ) immunotherapy induced microhemorrhages are associated with activated perivascular macrophages and peripheral monocyte recruitment in Alzheimer's disease mice. *Mol Neurodegener*. 2023;18:59. doi:10.1186/s13024-023-00649-w
22. Xu F, Guo M, Huang W, et al. Annexin A5 regulates hepatic macrophage polarization via directly targeting PKM2 and ameliorates NASH. *Redox Biol*. 2020;36(101634). doi:10.1016/j.redox.2020.101634
23. Xu X, Gao W, Li L, et al. Annexin A1 protects against cerebral ischemia-reperfusion injury by modulating microglia/macrophage polarization via FPR2/ALX-dependent AMPK-mTOR pathway. *J Neuroinflammation*. 2021;18:119. doi:10.1186/s12974-021-02174-3
24. Wang S, Sun Z, Zhao W, et al. CD97/ADGRE5 Inhibits LPS Induced NF-κB Activation through PPAR-γ Upregulation in Macrophages. *Mediators Inflamm*. 2016;2016:1605948. doi:10.1155/2016/1605948
25. Guilliams M, Thierry GR, Bonnardel J, Bajenoff M. Establishment and maintenance of the macrophage niche. *Immunity*. 2020;52:434–451. doi:10.1016/j.immuni.2020.02.015
26. Wan R, Srikaram P, Xie S, et al. PPARγ attenuates cellular senescence of alveolar macrophages in asthma-COPD overlap. *Respir Res*. 2024;25:174. doi:10.1186/s12931-024-02790-6
27. He S, Tian R, Zhang X, et al. PPARγ inhibits small airway remodeling through mediating the polarization homeostasis of alveolar macrophages in COPD. *Clin Immunol*. 2023;250:109293. doi:10.1016/j.clim.2023.109293
28. Cheng HS, et al. Exploration and development of PPAR modulators in health and disease: an update of clinical evidence. *Int J Mol Sci*. 2019;20. doi:10.3390/ijms20205055
29. Rehan VK, Liu J, Sakurai R, Torday JS. Perinatal nicotine-induced transgenerational asthma. *Am J Physiol Lung Cell Mol Physiol*. 2013;305:L501–507. doi:10.1152/ajplung.00078.2013
30. Rehman K, Tahir A, Niaz S, et al. Frequency of PPAR-γ, FTO and ABCC8 genetic variation in Pakistani cardiovascular smokers. *Environ Sci Pollut Res Int*. 2020;27:42611–42620. doi:10.1007/s11356-020-10226-z
31. Matheson J, Le Foll B. Therapeutic potential of Peroxisome Proliferator-Activated Receptor (PPAR) agonists in substance use disorders: a synthesis of preclinical and human evidence. *Cells*. 2020;9:1196. doi:10.3390/cells9051196
32. Qiu JF, Ma N, He Z-Y, et al. Erythromycin inhibits cigarette smoke-induced inflammation through regulating the PPARγ/NF-κB signaling pathway in macrophages. *Int Immunopharmacol*. 2021;96:107775. doi:10.1016/j.intimp.2021.107775
33. Wright MB, Bortolini M, Tadayyon M, Bopst M. Minireview: challenges and opportunities in development of PPAR agonists. *Mol Endocrinol*. 2014;28:1756–1768. doi:10.1210/me.2013-1427
34. Camp HS, Li O, Wise SC, et al. Differential activation of peroxisome proliferator-activated receptor-gamma by troglitazone and rosiglitazone. *Diabetes*. 2000;49:539–547. doi:10.2337/diabetes.49.4.539
35. Weidner C, de Groot JC, Prasad A, et al. Amorfrutins are potent antidiabetic dietary natural products. *Proc Natl Acad Sci U S A*. 2012;109:7257–7262. doi:10.1073/pnas.1116971109
36. Oppi S, Nusser-Stein S, Blyszczuk P, et al. Macrophage NCOR1 protects from atherosclerosis by repressing a pro-atherogenic PPARγ signature. *Eur Heart J*. 2020;41:995–1005. doi:10.1093/eurheartj/ehz667
37. Sen K, Pati R, Jha A, et al. NCoR1 controls immune tolerance in conventional dendritic cells by fine-tuning glycolysis and fatty acid oxidation. *Redox Biol*. 2023;59:102575. doi:10.1016/j.redox.2022.102575
38. Blondrath K, Steel JH, Katsouri L, et al. The nuclear cofactor receptor interacting protein-140 (RIP140) regulates the expression of genes involved in Aβ generation. *Neurobiol Aging*. 2016;47:180–191. doi:10.1016/j.neurobiolaging.2016.08.003
39. Liu M, Liu H, Liang F, Song XQ, Hu PA. Neuropeptide Y promotes adipogenic differentiation in primary cultured human adipose-derived stem cells. *Endocr J*. 2018;65:43–52. doi:10.1507/endocrj.EJ17-0017
40. Wu W, Hu P, Liang F, Song X, Liu M. High-dose neuropeptide Y inhibits proliferation and promotes differentiation of human adipose-derived stem cells. *Xi Bao Yu Fen Zi Mian Yi Xue Za Zhi*. 2016;32:185–190.
41. Wagner G, Fenzl A, Lindroos-Christensen J, et al. LMO3 reprograms visceral adipocyte metabolism during obesity. *J Mol Med*. 2021;99:1151–1171. doi:10.1007/s00109-021-02089-9
42. Yamamuro T, Nakamura S, Yanagawa K, et al. Loss of RUBCN/rubicon in adipocytes mediates the upregulation of autophagy to promote the fasting response. *Autophagy*. 2022;18:2686–2696. doi:10.1080/15548627.2022.2047341
43. Wang W, Ren W, Zhu L, Hu Y, Ye C. Identification of genes and key pathways underlying the pathophysiological association between sarcopenia and chronic obstructive pulmonary disease. *Exp Gerontol*. 2024;187:112373. doi:10.1016/j.exger.2024.112373
44. Chen Q, Shao X, He Y, et al. Norisoboldine attenuates sepsis-induced acute lung injury by modulating macrophage polarization *via* PKM2/HIF-1α/PGC-1α pathway. *Biol Pharm Bull*. 2021;44:1536–1547. doi:10.1248/bpb.b21-00457
45. Wang S, He N, Xing H, et al. Function of hesperidin alleviating inflammation and oxidative stress responses in COPD mice might be related to SIRT1/PGC-1α/NF-κB signaling axis. *J Recept Signal Transduct Res*. 2020;40:388–394. doi:10.1080/10799893.2020.1738483
46. Zhou J, Singh BK, Ho JP, et al. MED1 mediator subunit is a key regulator of hepatic autophagy and lipid metabolism. *Autophagy*. 2021;17:4043–4061. doi:10.1080/15548627.2021.1899691
47. Xu W, et al. Identification of a Potential PPAR-related multigene signature predicting prognosis of patients with hepatocellular carcinoma. *PPAR Res*. 2021:6642939.doi: 10.1155/2021/6642939.
48. Eapen MS, Hansbro PM, McAlinden K, et al. Abnormal M1/M2 macrophage phenotype profiles in the small airway wall and lumen in smokers and chronic obstructive pulmonary disease (COPD). *Sci Rep*. 2017;7:13392. doi:10.1038/s41598-017-13888-x
49. Byers DE, Wu K, Dang-Vu G, et al. Triggering receptor expressed on myeloid cells-2 expression tracks with M2-like macrophage activity and disease severity in COPD. *Chest*. 2018;153:77–86. doi:10.1016/j.chest.2017.09.044
50. Cornwell WD, Kim V, Fan X, et al. Activation and polarization of circulating monocytes in severe chronic obstructive pulmonary disease. *BMC Pulm Med*. 2018;18:101. doi:10.1186/s12890-018-0664-y
51. Hou C, Yan L, Sun K, et al. Nuclear receptor corepressor 1 deficiency exacerbates asthma by modulating macrophage polarization. *Cell Death Discov*. 2023;9:429. doi:10.1038/s41420-023-01724-3
52. Chen F, Li J, Zheng T, Chen T, Yuan Z. KLF7 alleviates atherosclerotic lesions and inhibits glucose metabolic reprogramming in macrophages by regulating HDAC4/miR-148b-3p/NCOR1. *Gerontology*. 2022;68:1291–1310. doi:10.1159/000524029

53. Yin F, Wu -M-M, Wei X-L, et al. Hepatic NCoR1 deletion exacerbates alcohol-induced liver injury in mice by promoting CCL2-mediated monocyte-derived macrophage infiltration. *Acta Pharmacol Sin*. 2022;43:2351–2361. doi:10.1038/s41401-022-00863-0
54. Yi ZJ, Gong JP, Zhang W. Transcriptional co-regulator RIP140: an important mediator of the inflammatory response and its associated diseases (Review). *Mol Med Rep*. 2017;16:994–1000. doi:10.3892/mmr.2017.6683
55. Zhang X, Li X, Jia H, An G, Ni J. The m(6)A methyltransferase METTL3 modifies PGC-1α mRNA promoting mitochondrial dysfunction and oxLDL-induced inflammation in monocytes. *J Biol Chem*. 2021;297:101058. doi:10.1016/j.jbc.2021.101058
56. Larson-Casey JL, Gu L, Davis D, et al. Post-translational regulation of PGC-1α modulates fibrotic repair. *FASEB J*. 2021;35:e21675. doi:10.1096/fj.202100339R
57. Qin L, Wu Y-L, Toneff MJ, et al. NCOA1 Directly Targets M-CSF1 expression to promote breast cancer metastasis. *Cancer Res*. 2014;74:3477–3488. doi:10.1158/0008-5472.Can-13-2639
58. Sandhu KK, Scott A, Tatler AL, Belchamber KBR, Cox MJ. Macrophages and the microbiome in chronic obstructive pulmonary disease. *Eur Respir Rev*. 2024;33:240053. doi:10.1183/16000617.0053-2024
59. Xue J, Schmidt S, Sander J, et al. Transcriptome-based network analysis reveals a spectrum model of human macrophage activation. *Immunity*. 2014;40:274–288. doi:10.1016/j.immuni.2014.01.006
60. He S, Xie L, Lu J, Sun S. Characteristics and potential role of M2 macrophages in COPD. *Int J Chron Obstruct Pulmon Dis*. 2017;12:3029–3039. doi:10.2147/copd.S147144